$(e,3e)$ process on a quantum dot

M. K. Srivastava
Institute Instrumentation Centre, Indian Institute of Technology, Roorkee, 247 667 (Uttaranchal), India
(Received 15 July 2004; published 1 December 2004)

The exact initial state wave function of an interacting electron pair in a quantum dot under parabolic confinement and neutralization of the dot by the substrate after ejection of electrons is exploited to obtain the fivefold differential cross section (X) of the $(e,3e)$ process on the dot. The reflections of the center-of-mass (c.m.) motion and relative motion on X are decoupled if the incident and scattered electrons are energetic and the ejected electrons are slow. The results are studied in fixed mutual angle (with zero c.m. momentum K) and Bethe ridge modes which allow the "cleanest" analysis of the contribution of the relative motion. The Coulomb interaction between the emitted electrons is found to qualitatively change the angular distribution of X. In the mode in which the magnitude of K is equal to the momentum transfer q, the angular distribution of X with respect to $\theta_{Kq}=\cos^{-1}(\hat{K}\cdot\hat{q})$ leads to a mapping of the initial c.m. wave function of the ejected pair. However, the c.m. motion is found to be best studied in the kinematics where the relative momentum $\vec{k}$ of the ejected pair is equal to $\vec{q}$.

DOI: 10.1103/PhysRevA.70.062702 PACS number(s): 34.80.Dp, 73.21.La

I. INTRODUCTION

The study of the effects of electron-electron correlations mediated through Coulomb interaction is one of the main aims in most atomic physics calculations. Two such processes which specifically aim to probe electron-electron correlations in the target are photo-double-ionization (γ-$2e$) and electron-impact double ionization $(e,3e)$. The calculation of this process as well as any other dealing with e-e correlations involves several approximations, as the problem does not have an exact solution. For example, any calculation of an (e-$3e$) process on any atomic target involves a target initial-state wave function that is approximate and more importantly a description of the final state that has more than two charged particles. This state does not have an exact solution. It is usually described through the use of effective charges which are supposed to mimic mutual Coulomb interactions [1–3]. Several sets of effective charges have been proposed. Another approach is to employ multi-Coulomb wave functions which give the correct asymptotic description to the final state [4–6]. Care has to be exercised so that these or any other approximation do not introduce features which mask the real physical ones of the process. One should look for models/situations which are either exactly solvable or require a different set of approximations.

Quantum dots provide such a situation. Semiconductor nanocrystals with nearly spherical boundaries can be thought of as artificial atoms where the confining potential replaces the potential of the nucleus. These have been experimentally realized by several workers. For example, Drexler *et al.* [7] prepared quantum dots in $GaAs/Al_xGa_{1-x}As$ and Hertmann *et al.* [8] in $In_xGa_{1-x}As/GaAs/AlAs$. It is believed that in these dots the electrons are confined by a potential that is quadratic when the number of electrons is small. For such a parabolic confinement, the two-electron states with full electron-electron Coulomb interaction can be found without any approximation. The details are given in the papers by Taut [9], Taut *et al.* [10], and Mandal *et al.* [11]. The center-of-mass and relative motions separate out in the same way as for free electrons. The photoejection of a correlated pair from a quantum dot has recently been considered by Fominykh *et al.* [12].

We consider the (e-$3e$) process initiated by an energetic electron ($\sim$200 eV) on a single quantum dot. The incident and scattered electrons may be described by plane waves. The role of the projectile is only to impart energy and momentum. The wave function of the two low-energy ejected electrons with full mutual Coulomb interaction can be obtained exactly without any approximation. In the next section we briefly describe for the sake of continuity the method to obtain the two-electron wave function in the quantum dot following Ref. [9]. The description of the two-electron final state is given in Sec. III. The expression for the scattering amplitude is obtained in Sec. IV. Section V contains the results.

II. TWO-ELECTRON WAVE FUNCTION IN A QUANTUM DOT

The Hamiltonian for two interacting electrons with coordinates $\vec{r}_1$ and $\vec{r}_2$ with respect to the center of the quantum dot in a parabolic confining potential of frequency ω,

$$H=-\frac{1}{2}\nabla_1{}^2-\frac{1}{2}\nabla_2{}^2+\frac{1}{2}\omega^2 r_1^2+\frac{1}{2}\omega^2 r_2^2+\frac{1}{|\vec{r}_1-\vec{r}_2|}, \quad (1)$$

can be expressed as a sum of two independent parts,

$$H=-\frac{1}{4}\nabla_R{}^2-\nabla_r{}^2+\frac{1}{4}\omega^2 r^2+\omega^2 R^2+\frac{1}{r}\equiv H_R+H_r, \quad (2)$$

by the transformation to center-of-mass (c.m.) and relative coordinates

$$\vec{R}=\frac{1}{2}(\vec{r}_1+\vec{r}_2), \quad \vec{r}=\vec{r}_1-\vec{r}_2. \quad (3)$$

We have used atomic units $\hbar=m=e=1$. The two-electron wave function can now be written as

$$\Phi(\vec{r}_1,\vec{r}_2) = \varphi(\vec{r})\xi(\vec{R})\chi(\vec{s}_1,\vec{s}_2) \tag{4}$$

because H is independent of spin. If the spin part χ is a triplet (singlet) state, then φ must be antisymmetric (symmetric) against particle exchange. There is no constraint on $\xi(\vec{R})$ because $\vec{R}$ is symmetric under exchange. The total energy is given by the sum of the eigenvalues E_R and E_r of H_R and H_r, respectively,

$$E = E_R + E_r. \tag{5}$$

The wave functions $\xi(\vec{R})$ and $\varphi(\vec{r})$ satisfy the equations

$$\left[-\frac{1}{2}\nabla_R{}^2 + \frac{1}{2}\omega_R{}^2 R^2\right]\xi(\vec{R}) = E'_R\xi(\vec{R}), \tag{6}$$

where $\omega_R = 2\omega$ and $E'_R = 2E_R$, and

$$\left[-\frac{1}{2}\nabla_r{}^2 + \frac{1}{2}\omega_r{}^2 r^2 + \frac{1}{2r}\right]\varphi(\vec{r}) = E'_r\varphi(\vec{r}), \tag{7}$$

where $\omega_r = \omega/2$ and $E'_r = E_r/2$. Equation (6) is the standard three-dimensional harmonic oscillator Schrödinger equation whose eigensolutions and eigenenergies for quantum members N and L are

$$\xi_{NLM}(\vec{R}) = \aleph_{NL} e^{-\eta^2/2}\eta^L {}_1F_1\left(-N, L+\frac{3}{2}, \eta^2\right)Y_{LM}(\hat{R}),$$

$$\eta = \omega_R{}^{1/2}R, \tag{8}$$

$$E'_R(N,L) = (2N + L + 3/2)\omega_R, \tag{9}$$

where $\aleph_{NL}$ is the normalization constant. Equation (7) for the relative motion admits solutions of the form

$$\varphi_{nlm}(\vec{r}) = \rho^l e^{-\rho^2/2}\upsilon_{nl}Y_{lm}(\hat{\rho}), \quad \rho = \omega_r{}^{1/2}r, \tag{10}$$

where υ_{nl} satisfies the equation

$$\left[\frac{d^2}{d\rho^2} + 2\left(\frac{l+1}{\rho} - \rho\right)\frac{d}{d\rho} + \epsilon'_{nl} - 2l - 3 - \frac{1}{\omega_r{}^{1/2}\rho}\right]\upsilon_{nl}(\rho) = 0, \tag{11}$$

which admits a series solution

$$\upsilon_{nl}(\rho) = \sum_{p=0} a_p\rho^p. \tag{12}$$

The energy ϵ'_{nl} is given by

$$\epsilon'_{nl} = 2E'_r(n,l)/\omega_r. \tag{13}$$

Equation (11) can be solved numerically and in special cases has an analytical solution. We have adopted the latter approach. The details are given in Ref. [9].

For the series (12) to terminate at ρ^{n-1}

$$\ldots a_{n-2} \neq 0,\ a_{n-1} \neq 0,\ a_n = 0,\ a_{n+1} = 0, \ldots. \tag{14}$$

The conditions (14) lead to the eigenvalue

$$\epsilon'_{nl} = 2n + 2l + 1 \tag{15}$$

and an (n,l)-dependent value for ω_r. For example, if $n=5$ and $l=0$, $\epsilon'_{nl}=11$ and the condition for $a_5=0$ leads to the equation

$$2848\omega_r^2 - 140\omega_r + 1 = 0 \tag{16}$$

for ω_r. The roots of this equation are

$$\omega_r = 0.008\,673\,102,\ \ 0.040\,484\,19.$$

We have used these values of n and l and $\omega_r = 0.008\,673\,102$ for the following reason. For this value of ω_r, the frequency ω of the confining parabolic potential of the quantum dot is 0.017 346 20. This leads to a spatial extent of the wave function of order 100 Å which is a typical size of a quantum dot. This combination of values of n and l is needed to obtain an analytical solution and typical quantum dot size.

Putting together Eqs. (10)–(12) and (15), the wave function $\varphi(\vec{r})$ for relative motion is given by

$$\varphi(\vec{r}) = \frac{a_0}{\sqrt{4\pi}}e^{-\rho^2/2}(1 + a_1\rho + a_2\rho^2 + a_3\rho^3 + a_4\rho^4), \tag{17}$$

where

$$a_1 = \frac{1}{2\sqrt{\omega_r}}, \tag{18}$$

$$a_2 = \frac{(1/2\omega_r - 8)}{6} \tag{19}$$

$$a_3 = \frac{(1/6\omega_r - 26/3)}{24\sqrt{\omega_r}}, \tag{20}$$

$$a_4 = \frac{1}{120}\left(\frac{1}{24\omega^2_r} - \frac{25}{6\omega_r} + 32\right). \tag{21}$$

The spin part χ of the wave function is a singlet state. The total energy E is given by

$$E = E_R + E_r = \omega(2N + L + n + l + 2). \tag{22}$$

We would like to point out that infinite harmonic oscillator confinement is an idealization and is needed for separability of the c.m. and relative motion parts of the wave function. However, it is expected that the low-lying states in the case of a finite harmonic confinement will not differ much from the corresponding infinite case.

III. TWO-ELECTRON WAVE FUNCTION IN THE FINAL STATE

The final state of the two ejected electrons with momenta $\vec{k}_b$ and $\vec{k}_c$ is described by

$$\Psi(\vec{r}_1,\vec{r}_2) = (2\pi)^{-3} e^{i\vec{k}_b\cdot\vec{r}_1} e^{i\vec{k}_c\cdot\vec{r}_2} e^{-\pi\alpha/2}\Gamma(1-i\alpha)_1 \times F_1(i\alpha,1,-ikr-i\vec{k}\cdot\vec{r}) = \psi(\vec{K},\vec{R})\psi_c(\vec{k},\vec{r}), \tag{23}$$

where

$$\psi(\vec{K},\vec{R}) = (2\pi)^{-3/2} e^{-\vec{K}\cdot\vec{R}}, \tag{24}$$

$$\psi_c(\vec{k},\vec{r}) = (2\pi)^{-3/2} e^{-\pi\alpha/2}\Gamma(1-i\alpha) e^{i\vec{k}\cdot\vec{r}}\, {}_1F_1(i\alpha,1,-ikr-i\vec{k}\cdot\vec{r}), \tag{25}$$

$$\vec{K} = \vec{k}_b + \vec{k}_c, \quad \vec{k} = \frac{1}{2}(\vec{k}_b - \vec{k}_c), \tag{26}$$

$$\alpha = 1/k. \tag{27}$$

The justification for this form of $\Psi(\vec{r}_1,\vec{r}_2)$ is that after ejection of electrons the quantum dot quickly becomes neutralized by the substrate, so that the final-state interaction between the two ejected electrons and the ionized quantum dot is effectively reduced to a two-body interaction between the free ejected electrons. This approximation has also been used by Fominykh *et al.* [12]. The interaction between the fast scattered electron and the slow ejected electrons has been ignored.

IV. SCATTERING AMPLITUDE

The scattering amplitude for the process in which an energetic electron of energy (momentum) E_i $(\vec{k}_i)$ is scattered with almost the same energy (momentum) E_a $(\vec{k}_a)$ and two low-energy electrons are ejected with energies E_b and E_c and momenta $\vec{k}_b$ and $\vec{k}_c$, respectively, is given by

$$F = -\frac{1}{2\pi}\left\langle e^{i\vec{k}_a\cdot\vec{r}_0}\Psi(\vec{r}_1,\vec{r}_2)\left|\frac{1}{r_{01}}+\frac{1}{r_{02}}\right|\Phi(\vec{r}_1,\vec{r}_2)e^{i\vec{k}_i\cdot\vec{r}_0}\right\rangle. \tag{28}$$

The energy and momentum conservation equations are

$$E_i + E = E_a + E_b + E_c, \tag{29}$$

$$\vec{k}_i + \vec{P}_i = \vec{k}_a + \vec{k}_b + \vec{k}_c, \tag{30}$$

where $\vec{P}_i$ $(=\vec{p}_1+\vec{p}_2)$ is the initial total momentum of the ejected electrons. Now carrying out integration with respect to the projectile coordinate $\vec{r}_0$ in Eq. (28) and using

$$e^{i\vec{q}\cdot\vec{r}_1} + e^{i\vec{q}\cdot\vec{r}_2} = 2e^{i\vec{q}\cdot\vec{R}}\cos\left(\frac{\vec{q}\cdot\vec{r}}{2}\right) \tag{31}$$

and Eqs. (4) and (23), the scattering amplitude reduces to

$$F = \frac{-4}{q^2}\langle\psi(\vec{K},\vec{R})|e^{i\vec{q}\cdot\vec{R}}|\xi(\vec{R})\rangle\left\langle\psi_c(\vec{k},\vec{r})\left|\cos\left(\frac{\vec{q}\cdot\vec{r}}{2}\right)\right|\varphi(\vec{r})\right\rangle. \tag{32}$$

Here $\vec{q}=\vec{k}_i-\vec{k}_a$ is the momentum transfer. The first matrix element in Eq. (32) is the Fourier transform $\overline{\xi}(\vec{q}-\vec{K})$ defined by

$$\overline{\xi}(\vec{q}-\vec{K}) = (2\pi)^{-3/2}\int e^{i(\vec{q}-\vec{K})\cdot\vec{R}}\xi(\vec{R})d\vec{R}. \tag{33}$$

The second matrix element in Eq. (32), with use of the partial wave decomposition

$$\cos\left(\frac{\vec{q}\cdot\vec{r}}{2}\right) = 4\pi\sum_{\substack{s=0\\ \text{even}}}(-1)^{s/2} j_s\left(\frac{qr}{2}\right)\sum_p Y_{sp}(\hat{q})Y_{sp}{}^*(\hat{r}) \tag{34}$$

and

$$\Psi_c(\vec{k},\vec{r}) = (2\pi)^{-3/2}\sum_{s=0} i^s e^{-i\sigma_s}F_s(kr)\sum_p Y^*{}_{sp}(\hat{r})Y_{sp}(\hat{k}), \tag{35}$$

$$F_s(kr) = \frac{2^s e^{-\pi\alpha/2}\Gamma(s+1-i\alpha)}{(2s+1)!}e^{-ikr}(kr)^s \times {}_1F_1(s+1-i\alpha,2s+2,2ikr), \tag{36}$$

$$\sigma_s = \arg I(s+1+i\alpha)$$

reduces to

$$\frac{4\pi}{(2\pi)^{3/2}}\sum_{\substack{s=0\\ \text{even}}} e^{i\sigma_s}(2s+1)P_s(\cos\theta_{kq})\int_0^\infty F_s(kr)j_s\left(\frac{qr}{2}\right)\varphi(r)r^2dr = \zeta(\vec{q},\vec{k}). \tag{37}$$

Finally, the fivefold differential cross section (X) is given by

$$\frac{d^5\sigma}{dE_b dE_c d\Omega_a d\Omega_b d\Omega_c} = \frac{k_a k_b k_c}{k_i}|F|^2 = \frac{k_a k_b k_c}{k_i}\frac{16}{q^4}|\overline{\xi}(\vec{q}-\vec{K})|^2|\zeta(\vec{q},\vec{k})|^2. \tag{38}$$

The reflections of the initial c.m. motion and relative motion are decoupled. It may be pointed out that this decoupling and the simple analytic form of the final expression are results of the assumption of parabolic confinement in the quantum dot and neutralization of the dot by the substrate after ejection of electrons. For fixed q, keeping $\vec{K}$ $(\vec{k})$ fixed and varying $\vec{k}$ $(\vec{K})$, the angular distribution of X may be used to single out the effect of the initial-state relative (center-of-

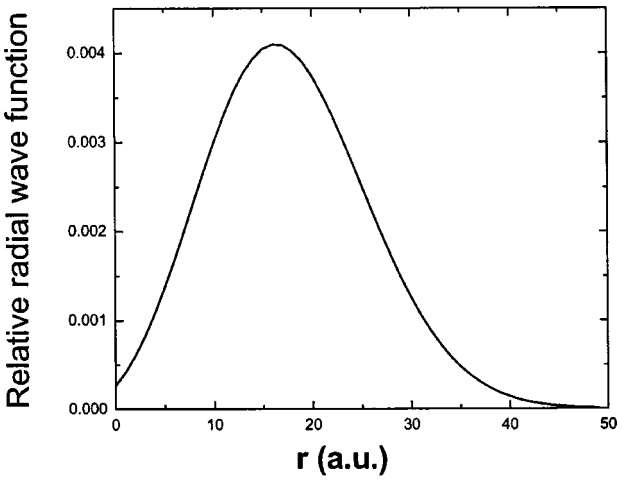

FIG. 1. Initial bound-state radial wave function $\varphi(r)$ with quantum numbers $n=5$, $l=0$ for relative motion.

mass) motion. Note that the wave function $\varphi(\vec{r})$ of relative motion defines the pair-correlation function $G(\vec{r}) \equiv |\varphi(\vec{r})|^2$ [9].

V. RESULTS

We have taken $n=5$, $l=0$, $m=0$ for the relative motion and have considered $N=0$, $L=0$, $M=0$ and $N=0$, $L=2$, $M=0$ for the c.m. motion in the initial state. Figures 1 and 2 show the radial wave functions $\varphi(r)$ and $\xi(R)$. We have considered 200-eV electrons scattered by the quantum dot with the scattered electrons taking away most of the energy while the ejected electrons are slow. In order to span whole range of variables $\vec{q}$, $\vec{k}_b$, and $\vec{k}_c$ the angular distribution of X has been studied in the literature in various kinematical arrangements, such as (i) fixed ejected angle mode, (ii) symmetrical emission mode, (iii) energy sharing with fixed total energy of ejected electrons mode, (iv) identical directions of emission and varying $\vec{q}$ mode, (v) fixed mutual angle mode, and (vi) Bethe ridge mode [2,3,13–17]. In the present study the c.m. contribution

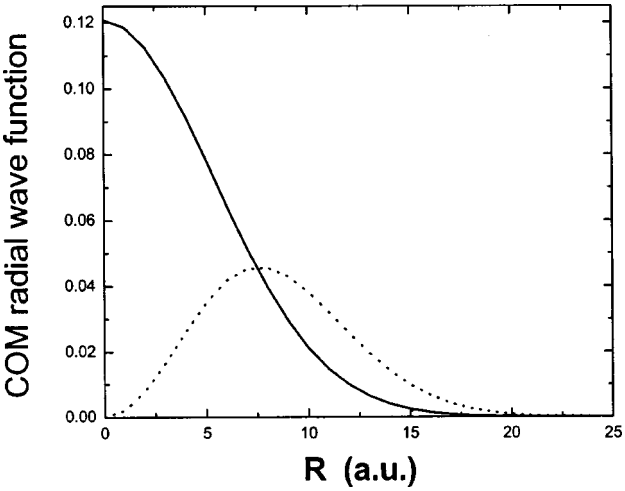

FIG. 2. Initial bound-state radial wave functions $\xi(R)$ with quantum numbers $N=0$, $L=0$ (—) and $N=0$, $L=2$ (···) for c.m. motion.

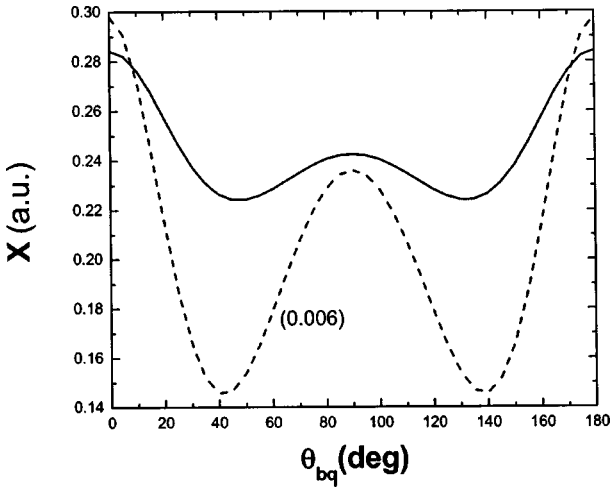

FIG. 3. Fivefold differential cross Section X for zero c.m. momentum ($K=0$) as a function of angle of emission θ_{bq} of the electron b with respect to momentum transfer direction at $E_i=200$ eV, $q=0.273$ a.u., and $E_b=E_c=5.0$ eV (——) and $E_b=E_c=2.5$ eV (---). The results at 2.5 eV have been multiplied by 0.006 to bring them on the same scale for comparison of angular distribution.

$$\frac{k_a k_b k_c}{k_i} |\overline{\xi}(\vec{q}-\vec{K})|^2$$

and the relative motion contribution

$$|\zeta(\vec{q},\vec{k})|^2$$

may be analyzed separately, and as the reflection of the electron-electron correlation is interesting, we have studied the angular distribution of X in the last two of the above kinematical arrangements in which the c.m. factor $|\overline{\xi}(\vec{q}-\vec{K})|^2$ is constant [$K=0$ or $\vec{q}=\vec{K}$]. Note that this is a first Born calculation with the aim of analyzing the angular distribution of X in the present context. The modifications caused by the Coulomb interaction between the scattered electron and the ejected electrons [18] and the second-order effects [19–21] have not been considered.

Figure 3 presents angular distribution in the fixed mutual angle mode, that is, with variable θ_b and θ_c while keeping the mutual angle θ_{bc} fixed for $L=0$. We have taken $\theta_{bc}=180°$ at $E_b=E_c=5.0$ and 2.5 eV and fixed $q=0.273$ a.u. The c.m. momentum K is now equal to zero and this makes $\overline{\xi}(\vec{q}-\vec{K}) \equiv \overline{\xi}(\vec{q})$ independent of θ_b or θ_c. A fixed value of $\vec{q}$ implies here a fixed value of $\vec{P}_i$ as $\vec{q}+\vec{P}_i=\vec{K}=0$. The c.m. motion in this kinematics therefore plays no role in the angular distribution of X, which is determined by the relative motion of b and c. In the case of a $(\gamma,2e)$ process, the cross section vanishes in this case [3]. The present results therefore manifest a nondipolar contribution. The cross section is symmetrical about $\theta_{bq}=90°$ because of the singlet initial state and can be represented as

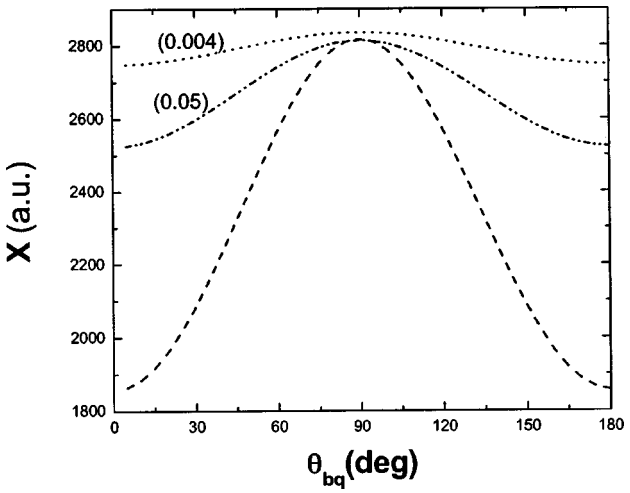

FIG. 4. Same as Fig. 3, but at $\theta_a=2°$ ($q=0.135$ a.u.), $E_b=E_c=2.5$ eV (---); $\theta_a=1°$ ($q=0.069$ a.u.), $E_b=E_c=2.5$ eV (-···-···-); and $\theta_a=0.5°$ ($q=0.037$ a.u.), $E_b=E_c=2.5$ eV (···). The results have been multiplied by the indicated factors to bring them on the same scale.

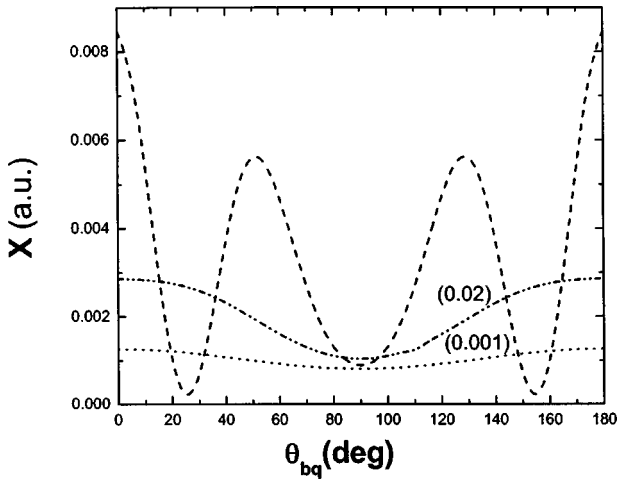

FIG. 5. Fivefold differential cross Section X with Coulomb interaction between the ejected electrons switched off in the final state for zero c.m. momentum ($K=0$) as a function of angle of emission θ_{bq} of the electron b with respect to momentum transfer direction for $E_i=200$ eV at $\theta_a=2°$, $E_b=E_c=2.5$ eV (---); $\theta_a=1°$, $E_b=E_c=2.5$ eV (-···-···-); and $\theta_a=0.5°$, $E_b=E_c=2.5$ eV (···). The results have been multiplied by the indicated factors to bring them on the same scale.

$$\left| \sum_{\lambda=0,\text{even}} A_\lambda(q,k) P_\lambda(\cos\theta_{kq}) \right|^2,$$

where q and k are constant. It shows a peak when one of the electrons is emitted along the momentum transfer direction and the other opposite to it, and a subsidiary peak at $\theta_{bq}=90°$ which corresponds to $\vec{k}_b \perp \vec{q}, \vec{k}_c \perp \vec{q}$ along with $\vec{k}_b = -\vec{k}_c$. This is in apparent accord with the observations of Lahmam-Bennani *et al.* [3,15] in the atomic case. This latter peak becomes more marked and the overall value of the cross section increases when E_b $(=E_c)$ decreases (Fig. 3). Both of these features are caused by the factor $|\zeta(\vec{q},\vec{k})|^2$. A decrease in momentum transfer, however, decreases the peak at $\theta_{bq}=90°$. The angular distribution of X for different values of q at $E_b=E_c=2.5$ eV is shown in Fig. 4. At $\theta_a=2°$ ($q=0.135$ a.u.), the ratio of maximum to minimum cross section is about 1.5, at $\theta_a=1°$ ($q=0.069$ a.u.) it is about 1.1, while at $\theta_a=0.5°$ ($q=0.037$ a.u.) it is only about 1.03. The results have been multiplied by suitable factors to bring them on the same scale for comparison of the angular distribution. The large variation with q requiring this scaling is here due to the constant q-dependent factor $|\bar{\xi}(\vec{q})|^2$ in X; the angular distribution is, however, controlled by $|\zeta(\vec{q},\vec{k})|^2$. We thus find that the overall magnitude of the relative motion factor $|\zeta(\vec{q},\vec{k})|^2$ in X mainly depends on k while its angular distribution depends on both k and q. At low values of q and k, the differential cross section is essentially contributed by $\lambda=0,2$ with the coefficients A_0 and A_2 having opposite signs. The Coulomb interaction between the two electrons in the final state favors symmetrical emission which in the $K=0$ geometry corresponds to $\theta_{bq}=\theta_{cq}=90°$. If it is ignored, the angular distribution of X shows a minimum at $\theta_{bq}=90°$ (Fig. 5). This minimum becomes shallower as q decreases. The ratios of the cross section at $\theta_{bq}=0°$ to the cross section at $\theta_{bq}=90°$ are about 11, 2.8, and 1.6 at $q=0.135$, 0.069, and 0.037, respectively. The occurrence of the minimum indicates that the coefficients A_0 and A_2 now have the same sign. The differences in angular distribution of the results with and without Coulomb interaction (Figs. 4 and 5) in the final state very clearly demonstrate the importance of the final-state e-e correlation.

For fixed θ_{bq} $(\theta_{cq})=90°$ (say), the above kinematics ($K=0$) may also be used to span $\bar{\xi}(P_i)$ by varying $\vec{q}$. At these values, X is given by

$$\left.\frac{d^5\sigma}{dE_b dE_c d\Omega_a d\Omega_b d\Omega_c}\right|_{\theta_{bq}=90°} = \frac{32 k_a k_b k_c}{\pi k_i q^4} |\bar{\xi}(\vec{q})|^2 \left| \int_0^\infty F_0(kr) j_0(qr/2) \varphi(r) r^2 dr \right|^2, \quad (39)$$

where $\bar{\xi}(\vec{q})$ for $L=0$ is given by

$$\bar{\xi}(\vec{q}) = (\pi\omega_R)^{-3/4} \exp(-q^2/2\omega_R). \quad (40)$$

Figure 6 shows variation of $\ln[q^4 X]$ against q^2 for $E_b=E_c=2.5$ eV. Note that in this kinematics $\vec{q}+\vec{P}_i=0$. The straight line portion for small values of q corresponds to the region where $j_0(qr/2)$ is essentially equal to unity over the effective range of integration. For larger values of q, the curve lowers down as expected.

Figure 7 shows the results in the Bethe ridge kinematics [22] where momentum transfer $\vec{q}$ is equal to center-of-mass momentum $\vec{K}$ $(=\vec{k}_b+\vec{k}_c)$. The values of θ_b, θ_c, E_b, E_c, and θ_{kq} under Bethe ridge conditions for different values of θ_{bc} and given E_b+E_c may be obtained easily from energy/momentum conservation relations [Eqs. (29) and (30)]. This kinematics corresponds to the initial total momentum P_i equal to zero. In the present case where c.m. and relative

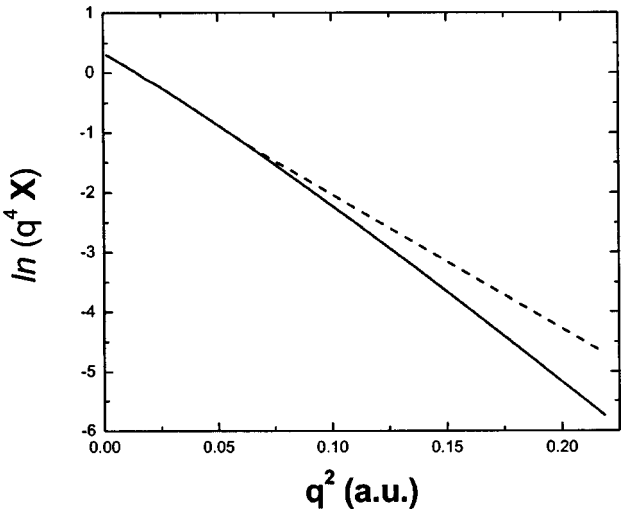

FIG. 6. Plot of $\ln[q^4X]$ as a function of q^2 for $E_i=200$ eV and $E_b=E_c=2.5$ eV in the $K=0$ kinematics at fixed $\theta_{bq}=\theta_{cq}=90°$. Dashed line is extrapolation of the initial straight line portion.

motions are decoupled, the angular distribution of X depends only on the relative motion as the factor $\overline{\xi}(\vec{q}-\vec{K})\equiv\overline{\xi}(0)$ is a nonzero constant for $L=0$. It is found that X is maximum when the more energetic of the two electrons is emitted near the momentum transfer direction and the other one nearly opposite to it. Similar results have been obtained earlier by Srivastava *et al.* [2] in the case of $(e,3e)$ on helium by energetic electrons using the Hartree-Fock wave function of Byron and Joachain [23] and "open-shell" wave function of Silvermann *et al.* [24] for the helium ground state. This event corresponds to a binary collision in which one electron is emitted near the momentum transfer direction and the other one by shake-off. This has a higher probability. As the energetic electron moves away from the $\hat{q}$ direction and θ_{bc} decreases (or θ_{kq} increases), the cross section decreases. The Coulomb repulsion between b and c also contributes to this

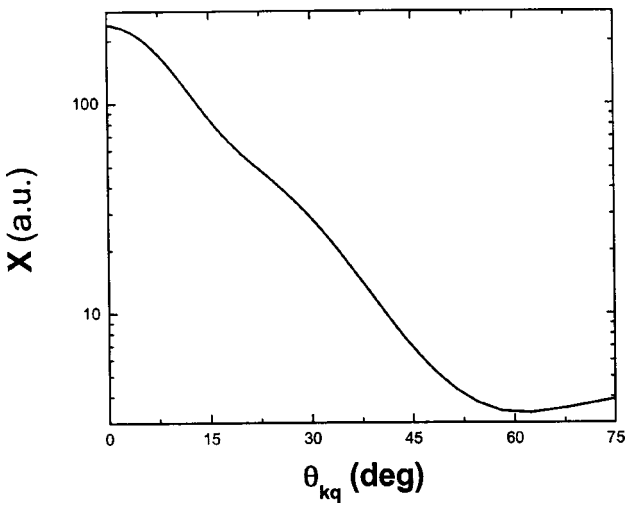

FIG. 7. Fivefold differential cross Section X in Bethe ridge kinematics for $E_i=200$ eV, $E_b+E_c=10$ eV at $\theta_a=10°$ ($q=0.666$ a.u.) as a function of angle θ_{kq} between the directions of relative motion $\vec{k}$ and momentum transfer $\vec{q}$. The c.m. and relative momenta K and k are equal to 0.666 a.u. and 0.507 a.u., respectively.

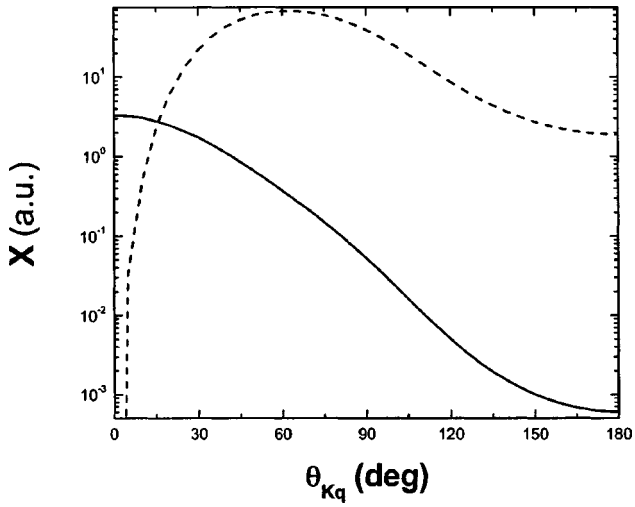

FIG. 8. Fivefold differential cross Section X in fixed mutual angle mode $\theta_{bc}=2\cos^{-1}(q/2k_b)$ as a function of $\theta_{Kq}=\cos^{-1}(\vec{q}\cdot\vec{K})$ at $E_i=200$ eV, $\theta_a=4°$, $E_b=E_c=5.0$ eV. The magnitudes of c.m. momentum K and momentum transfer q are equal. The quantum numbers of the initial c.m. wave functions are $N=0$, $L=0$ (—) and $N=0$, $L=2$ (---).

decrease. Note that there is no Bethe ridge contribution for $L\neq 0$ because in this case the probability of having $P_i=0$ vanishes.

Let us now consider equal energy of emission, $E_b=E_c$ (=5.0 eV), under Bethe ridge conditions and take

$$\theta_{bc}=2\cos^{-1}(q/2k_b), \tag{41}$$

so that $q=K$. Now if X is considered in fixed mutual angle (at this value of θ_{bc}) mode as a function of θ_{Kq} $\{=\cos^{-1}(\hat{K}\cdot\hat{q})\}$, it spans the c.m. momentum distribution $\overline{\xi}[2q\sin(\theta_{Kq}/2)]$ of the ejected electrons in the initial state. This kinematics has been considered earlier by Lahmam-Bennani *et al.* [17]. Figure 8 shows this for the initial c.m. states with quantum numbers $(N=0,L=0)$ and $(N=0,L=2)$. The cross section is zero at $\theta_{Kq}=0$ in the case of $L=2$. It should be noted that the factor $\zeta(\vec{q},\vec{k})$ in X is not constant here and affects the angular distribution. The separation between the contributions of the c.m. and relative motions is therefore not "clean."

Figures 9 and 10 show our results for fixed E_b+E_c as a function of $|\vec{q}-\vec{K}|$ in a new kinematical arrangement where the relative momentum $\vec{k}$ is equal to the momentum transfer $\vec{q}$. This makes the relative motion factor $\zeta(\vec{q},\vec{k})\equiv\zeta(\vec{q},\vec{q})$ in X a constant. The values of $E_b,E_c,\theta_b,\theta_c,\theta_{kq}$ and $q-K$ in this arrangement for given values of θ_{bc}, E_b+E_c, θ_a, and E_i may be obtained from energy/momentum conservation relations [Eqs. (29) and (30)] as before. The variation of X here is essentially given by the c.m. factor which is the Fourier transform of the initial-state c.m. wave function of the ejected pair.

VI. SUMMARY

The structure of the fivefold differential cross section (X) as a product of two factors depending on c.m. motion and

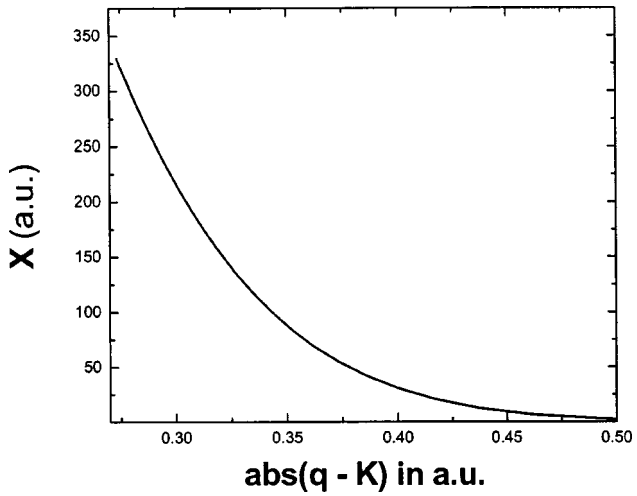

FIG. 9. Fivefold differential cross Section X as a function of $|\vec{q}-\vec{K}|$ in the kinematics where $\vec{k}=\vec{q}$ at $E_i=200$ eV, $\theta_a=4°$, and $E_b+E_c=10$ eV. The quantum numbers of the initial c.m. wave function are $N=0$, $L=0$.

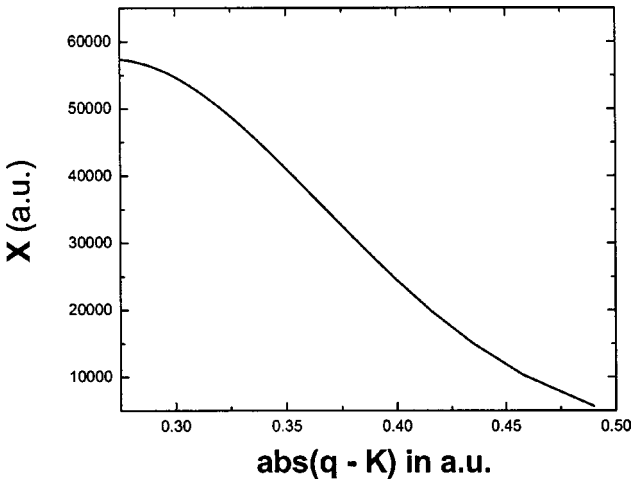

FIG. 10. Same as Fig. 9, but with $N=0$, $L=2$ initial c.m. wave function.

relative motion in the case of a quantum dot is exploited to analzse the reflections of the initial c.m. and relative motions on it separately. The kinematical arrangements where $\vec{K}=\vec{q}$ (Bethe ridge), $K=0$, and $\vec{k}=\vec{q}$ are found to be very useful in making one of the factors (depending on c.m. motion or depending on relative motion) a constant. These, for a given $\vec{q}$, correspond, respectively, to cases where the initial total momentum $\vec{P}_i$ of the two electrons is zero, has a fixed value $(=-\vec{q})$, or varies. The angular distribution of X in $K=0$ kinematics shows a very interesting manifestation of *e*-*e* Coulomb correlation in the final state and is found to be very useful in probing the initial bound-state relative motion wave function. It may also be used with varying q and fixed $\theta_{bq}=90°$ to probe the initial bound-state c.m. wave function for small P_i. The $K=q$ kinematics, though not providing a clean separation, is quite useful in probing the relative motion wave function.

ACKNOWLEDGMENTS

This work was supported by the Council of Scientific and Industrial Research, Government of India, under Project No. 21(0497) and the All India Council for Technical Education.

[1] J. Berakdar, Phys. Lett. A **220**, 238 (1996).
[2] M.K. Srivastava, S. Gupta, and C. Dal Cappello, Phys. Rev. A **53**, 4104 (1996).
[3] A. Lahmam-Bennani, I. Taouil, A. Duguet, M. Lecas, L. Avaldi, and J. Berakdar, Phys. Rev. A **59**, 3548 (1999).
[4] J. Berakdar, Phys. Rev. A **55**, 1994 (1997).
[5] A.W. Malcherek and J.S. Briggs, J. Phys. B **30**, 4449 (1997).
[6] A.W. Malcherek, J.M. Rost, and J.S. Briggs, Phys. Rev. A **55**, R3979 (1997).
[7] H. Drexler, D. Leonard, W. Hansen, J.P. Kotthaus, and P.M. Petroff, Phys. Rev. Lett. **73**, 2252 (1994).
[8] D. Heitmann, K. Bollweg, V. Gudmundsson, T. Kurth, and S.P. Riege, Physica E (Amsterdam) **1**, 204 (1997).
[9] M. Taut, Phys. Rev. A **48**, 3561 (1993).
[10] M. Taut, A. Ernst, and H. Eschrig, J. Phys. B **31**, 2689 (1998).
[11] S. Mandal, P.K. Mukherjee, and G.H.F. Diercksen, J. Phys. B **36**, 4483 (2003).
[12] N. Fominykh, O. Kidun, A. Ernst, and J. Berakdar, J. Phys. B **36**, 1 (2003).
[13] S. Gupta and M.K. Srivastava, Phys. Rev. A **52**, 2083 (1995).
[14] I. Taouil, A. Lahmam-Bennani, A. Duguet, and L. Avaldi, Phys. Rev. Lett. **81**, 4600 (1998).
[15] A. Lahmam-Bennani, A. Duguet, M.N. Gaboriaud, I. Taouil, M. Lecas, A. Kheifets, J. Berakdar, and C. Dal Cappello, J. Phys. B **34**, 3073 (2001).
[16] P. Golecki and H. Klar, J. Phys. B **34**, L779 (2001).
[17] A. Lahmam-Bennani, C.C. Jia, A. Duguet, and L. Avaldi, J. Phys. B **35**, L215 (2002).
[18] J.R. Gotz, M. Walter, and J.S. Briggs, J. Phys. B **36**, L77 (2003).
[19] A. Lahmam-Bennani, J. Phys. B **34**, 3073 (2001).
[20] M.K. Srivastava and Kshamata Muktavat, Pramana **58**, 647 (2002).
[21] A. Lahmam-Bennani, A. Dueget, C. Dal Cappello, H. Nebdi, and B. Piraux, Phys. Rev. A **67**, 010701 (2003).
[22] A. Lahmam-Bennani, J. Phys. B **24**, 2401 (1991).
[23] F. W. Byron, Jr. and C.J. Joachain, Phys. Rev. **146**, 1 (1966).
[24] J.N. Silvermann, O. Platas, and F.A. Matsen, J. Chem. Phys. **32**, 1402 (1960).